SHED-derived Exosomes Ameliorate Hyposalivation Caused by Sjögren Syndrome *via* Akt/GSK-3β/Slug-mediated ZO-1 Expression

Zhihao Du
Peking University School of Stomatology https://orcid.org/0000-0002-8973-761X
Pan Wei
Peking University School of Stomatology: Peking University Hospital of Stomatology
Nan Jiang
Peking University School of Stomatology: Peking University Hospital of Stomatology
Liling Wu
Peking University School of Basic Medical Sciences
Chong Ding (idtbbsb@163.com)
Peking University - School of Stomatology: Peking University Hospital of Stomatology
https://orcid.org/0000-0002-1834-4421
Guangyan Yu
Peking University School of Stomatology: Peking University Hospital of Stomatology

Research Article

Keywords: Stem cells from human exfoliated deciduous teeth, Exosomes, Saliva, Sjögren syndrome, Submandibular gland

Posted Date: February 10th, 2022

DOI: https://doi.org/10.21203/rs.3.rs-1305483/v1

Abstract

Objective: To explore the therapeutic role and mechanism of exosomes obtained from the supernatant of stem cells derived from human exfoliated deciduous teeth (SHED-exos) in sialadenitis caused by Sjögren syndrome (SS).

Methods: SHED-exos were administered to the submandibular glands (SMGs) of 14-week-old nonobese diabetic (NOD) mice, an animal model of the clinical phase of SS, by local injection or intraductal infusion. The saliva flow rate was measured after pilocarpine intraperitoneal injection in 21-week-old NOD mice. Protein expression was examined by Western blot analysis. Exosomal miRNAs were identified by microarray analysis. Paracellular permeability was evaluated by transepithelial electrical resistance measurement.

Results: Local injection of SHED-exos significantly increased saliva secretion and alleviated lymphocytic infiltration in the SMGs of NOD mice. The injected SHED-exos could be taken up by glandular epithelial cells and increased ZO-1 expression. Moreover, SHED-exos increased paracellular permeability, whereas this effect disappeared in ZO-1 knockout cells and reappeared in ZO-1-rescued cells. Furthermore, 180 exosomal miRNAs were identified from SHED-exos, and Kyoto Encyclopedia of Genes and Genomes (KEGG) analysis suggested that the PI3K/Akt pathway might play an important role. SHED-exos treatment induced the downregulation of p-Akt/Akt, p-GSK-3β/GSK-3β, and Slug and the upregulation of ZO-1 in SMGs and SMG-C6 cells. Both the increased ZO-1 expression and paracellular permeability induced by SHED-exos were abolished by IGF1, a PI3K agonist. In addition, Slug bound to the ZO-1 promoter and suppressed its expression. For safer and more effective clinical application, SHED-exos were intraductally infused into the SMGs of NOD mice, and saliva secretion was increased and accompanied by decreased levels of p-Akt/Akt, p-GSK-3β/GSK-3β, and Slug and increased ZO-1 expression.

Conclusion: Local application of SHED-exos in SMGs can ameliorate Sjögren syndrome-induced hyposalivation by increasing the paracellular permeability of glandular epithelial cells through Akt/GSK-3β/Slug pathway-mediated ZO-1 expression.

Introduction

Sjögren syndrome (SS) is a systemic autoimmune disease histopathologically characterized by lymphocytic infiltration of exocrine glands such as the salivary and lacrimal glands, leading to destruction and dysfunction present with sicca symptoms (dry mouth and dry eye) [1, 2]. According to the literature, more than 95% of SS patients present with sicca symptoms, accompanied with 70% of patients have systemic symptoms such as fatigue and musculoskeletal pain. Glandular dysfunction has a chronic course and might remain stable for a long period of time (up to 12 years) [3]. In addition, approximately 60% of SS patients coexist with other autoimmune diseases, such as rheumatoid arthritis and

autoimmune thyroid disease, which have an important impact on health-related quality of life and even worse, threaten life [4].

As a systemic autoimmune disease, the treatment of SS is still challenging. Traditional therapeutic schedules are focused on relieving sicca syndrome with artificial tears and saliva and even inducing their production [5]. Others are concentrated on suppressing the immune system with immunosuppressant and immunomodulatory drugs [6]. However, the former cannot repair the damaged glands and restore their function [5], and the long-term use of immunosuppressant drugs might increase the risk of infection and the incidence of metabolic disorders and result in cardiovascular disease [6, 7]. Recently, intravenous injection of bone marrow mesenchymal stem cells (BMMSCs), umbilical cord mesenchymal stem cells, stem cells from human exfoliated deciduous teeth (SHEDs), and conditioned media from dental pulp stem cells have been reported to alleviate the decreased saliva secretion in experimental and clinical SS [8, 9, 10]. Nevertheless, implanted mesenchymal stem cells (MSCs) will not survive for a long time *in vivo*, and the injected cells cannot migrate to the damaged glands [10, 11]. Moreover, the conditioned media contains numerous and diverse cytokines, and defining the exact factors that work is complex [9, 12, 13, 14]. Therefore, it is critical to determine an effective strategy that is easy to produce with stable performance and clear composition.

Exosomes are extracellular microvesicles with a diameter range of 30-150 nm that are positive for CD63 and HSP70 [15, 16]. Generally, exosomes are described as mini-maps of their cells of origin. In addition, compared with stem cells, exosomes have shown more potential advantages for clinical application, including (but not limited to) no need to be administered systemically and no self-replication [17]. Recently, exosomes have attracted great increasing attention in cell therapy. For example, the antitumor activities of MSCs are largely mediated through exosome-established multidirectional communication in the tumor microenvironment [18]. BMMSC-derived exosomes were found to induce long-term neuroprotection and promote neuroregeneration and neurological recovery in a rodent stroke model at the same time [19, 20]. Stem cell-derived exosomes improve ischemia/reperfusion injury in rat lungs [21]. Our recent study has shown that intravenous injection of SHEDs protects gland function, avoiding immune damage, in 7-week-old NOD mice, which represents an initial phase of SS [10]. However, with respect to patients in the clinical phase of SS displaying developed inflammation and gland dysfunction, whether SHED-derived exosomes (SHED-exos) have a therapeutic effect on sialadenitis, as well as the underlying mechanism, needs to be elucidated.

Therefore, the purposes of the present study were to explore the therapeutic effects of SHED-exos on the structure and functional injury caused by SS and to further reveal the underlying mechanism of increasing saliva secretion of the damaged glands by SHED-exos.

Materials And Methods

Cell and tissue culture

This study was approved by the institutional review board of Peking University School of Stomatology (PKUSSIRB-201950162). SHEDs were provided by the ORAL STEM CELL BANK (Beijing Tason Biotech Co., China) and cultured in MSC medium containing 10% fetal bovine serum (FBS), 100 μg/ml streptomycin and 100 U/ml penicillin. Human submandibular gland (SMG) tissues were obtained from 5 patients (45-58 years old; 3 females) who had primary oral squamous cell carcinoma but had not received irradiation and chemotherapy and were undergoing functional neck dissection as part of surgical treatment. All the collected tissues were histologically confirmed as normal. For acinar cell preparation, gland tissue was minced on ice and digested with collagenase (Worthington, Lakewood, NJ, USA) and 1% BSA for 60 min as reported previously [22]. Duct cells were cultured from Wharton's duct tissues with high expression of CK8 and low expression of α-amylase. Damaged labial gland samples were obtained from 5 SS patients (25-45 years old; 3 females, diagnosis according to the American College of Rheumatology/European League Against Rheumatism Criteria) in Peking University School of Stomatology, and the labial glands obtained from mucocele patients served as normal controls. The fresh gland tissues were minced into small pieces (0.5 mm^3) and cultured with or without SHED-exos for 24 h at 37 °C. Then, the tissues were collected for further examination. The rat submandibular epithelial cell line with characteristics of acinar cells (SMG-C6, a generous gift from Dr. David O. Quissell) was routinely cultured in Dulbecco's modified Eagle's medium (DMEM)/F12 (1:1 mixture) containing 5 μg/ml transferrin, 2 nM triiodothyronine, 1.1 μM hydrocortisone, 0.1 μM retinoic acid, 5 mM glutamine, 80 ng/ml epidermal growth factor, 50 μg/ml gentamicin sulfate, 5 μg/ml insulin, 100 U/ml penicillin, 100 μg/ml streptomycin, and 2.5% FBS [23]. All cell and tissue culture constituents were purchased from Gibco and Sigma–Aldrich.

Exosome isolation and identification

Exosomes were collected from the supernatants of SHEDs (cultured in exosome-free medium) and isolated by ultracentrifugation and sucrose cushion as described previously [24]. For identification, SHED-exos were stained with phosphotungstic acid and examined with a transmission electron microscope (JEM-1400 electron microscope). Furthermore, the size distribution and particle concentration were determined by nanoparticle tracking analysis (NTA) with a NanoSight NS300 (Malvern, UK) and 3.2 DevBuild 3.2.16.

SHED-exos treatment

The Peking University Institutional Review Board for the care and use of laboratory animals approved all the experiments in this study (LA2019109). 7- and14-week-old female NOD mice were obtained from Peking University Health Science Center. The investigation conformed to the Guide for the Care and Use of Laboratory Animals published by the US National Institutes of Health. All animal surgeries were performed under chloral hydrate (400 mg/kg body weight), and all efforts were made to minimize suffering. For injection, 50 μg SHED-exos (diluted in 25 μl PBS) were injected into the SMGs at multiple points in 14-week-old NOD mice, which represents the clinical phase of SS. For intraductal infusion, the intraoral duct orifice of the SMG was inserted with an Intrathecal Catheter System (11.7 cm, 32 g accepts,

27 g needles) and perfused with 50 μg SHED-exos into 14-week-old NOD mice. Equal volume of PBS was perfuse as control. Then, the mice were sacrificed until 21 weeks, and the SMGs were collected.

Stimulated saliva flow measurement

Under anesthesia, the mice were intraperitoneally injected with pilocarpine (0.05 mg/100 g body weight), and then the whole saliva was collected with a micropipette from the oral cavity for 10 min. The weight of the saliva was measured with a precision weighing balance (METTLER TOLEDO).

Histological evaluation

The SMG tissues of mice were surgically removed and fixed with 4% paraformaldehyde and embedded in paraffin wax. The specimens were serially cut into 5 μm thick sections and stained with hematoxylin and eosin. The sections were observed under a microscope for lymphocytic infiltration. The degree of inflammation was assessed by the focus score defined as the number of foci comprising ≥ 50 mononuclear cells per 4 mm^2 of gland tissue and the ratio index defined as the ratio of the foci area to the tissue total area.

SHED-exos labeling and tracking

SHED-exos were incubated with 1,1-dioctadecyl-3,3,3,3-tetramethylindotricarbocyanine iodide (DiR; Invitrogen) and PKH26 (Sigma–Aldrich) and then injected into the glands. The bioluminescence was measured using the IVIS Imaging System (Caliper Life Sciences). Next, PKH26-labeled SHED-exos were incubated with SMG-C6 cells, primary cultured human SMG acinar cells, and duct cells for 24 h. The above images were captured by confocal microscopy (LMS710, Carl Zeiss Microscopy).

Real-time PCR

Total RNA was extracted using TRIzol reagent (Invitrogen), and cDNA was synthesized using a cDNA Reverse Transcription Kit (Takara). PCR was conducted with FastStart Universal SYBR Green Master reagent (Roche) as described on the ABI Prism 7500 real-time PCR system (Applied Biosystems). The primer sequences are listed in Table S1.

Microarray analysis

SHED-exos were analyzed with an Agilent Human miRNA microarray (v21.0; Agilent Technologies Inc., Santa Clara, CA, USA). The original data files were processed by Feature Extraction software. Signals were normalized using Gene Spring GX software 11.0 (Agilent Technologies). The target genes underwent further Kyoto Encyclopedia of Genes and Genomes (KEGG) pathway classification analysis.

Western blot analysis

Gland tissues and SMG-C6 cells were harvested in lysis buffer (RIPA buffer, #89900, Thermo Fisher Scientific) and ultrasonicated at 4 °C for 30 s. After centrifugation at 12,000 g for 10 min, the protein

concentrations were determined using a bicinchoninic acid protein assay kit (MPK002; M&C Gene Technology). The proteins (30 μg) were separated by 12% SDS–PAGE, transferred to PVDF membranes, probed with primary antibodies, and then incubated with horseradish peroxidase-conjugated secondary antibodies (ZSGB-BIO). The target proteins were detected using enhanced chemiluminescence reagent (Huaxingbio). Detailed information on the antibodies is listed in Table S2. Immunoreactive band intensities were calculated with ImageJ software v1.8.0.

Transepithelial electrical resistance measurement

Confluent monolayers of SMG-C6 cells were grown in 24-well Corning Transwell™ chambers (Costar) for 7 days, and then transepithelial electrical resistance (TER) was measured at 37 °C using an Epithelial Volt Ohm Meter (EVOM; WPI, FL). TER values were calculated by subtracting the blank filter (90 Ω) and by multiplying the surface area of the filter.

ZO-1 knockout and rescue

SMG-C6 cells were transfected with the zonula occludens (ZO)-1 sgRNA plasmid (sequence: TTCACCAATGTGACCTTGGT; Genechem Inc.). Scrambled guide RNA plasmids were used as a negative control. For re-expression ('rescue'), ZO-1 knockout SMG-C6 cells were cultured to 60% confluency and transfected with ZO-1 cDNA plasmids (#30313, Addgene).

Double luciferase reporter gene assay

A rat ZO-1 promoter fragment was amplified by PCR and inserted into the pGL3 vector. HEK293T cells were transfected with plasmids expressing the ZO-1 promoter region or Slug. For normalization, the Renilla luciferase reporter construct was cotransfected. All luciferase assays were analyzed after 24 h of transfection using a Dual-Luciferase Kit (Promega) according to the manufacturer's protocol.

Statistical analysis

Data are shown as the mean ± SD. Statistical analysis was performed by unpaired Student's *t* test between two groups or two-way ANOVA followed by Bonferroni's test among multiple groups using Prism 6.0 software (GraphPad CA, USA). $P < 0.05$ was considered statistically significant.

Results

SHED-exos increase saliva secretion and ameliorate lymphocytic infiltration in the SMGs of NOD mice

SHED-exos extracted from SHEDs culture supernatant were identified and showed a standard microstructure (Figure 1A), and they expressed the exosome-associated proteins CD9, CD63, C81, and HSP70 (Figure 1B). The mean diameter of SHED-exos was 126.5±5.7 nm (Figure 1C). The stimulated saliva flow rate was significantly decreased in 14-week-old NOD mice and further dropped in 21-week-old NOD mice compared with 7-week-old NOD mice and age-matched BALB/c mice (Figure 1D). To explore

the therapeutic effect of SHED-exos on sialadenitis, we injected 50 μg SHED-exos into the SMGs of 14-week-old NOD mice and sacrificed the mice at 21 weeks. SHED-exos significantly increased the stimulated saliva flow rate compared with those in age-matched untreated and PBS-treated groups. Moreover, quantitative analysis showed that the focus score and the ratio index were increased in 21-week-old NOD mice, but both of them were significantly decreased in the SHED-exo-treated group compared with the age-matched untreated and PBS-treated groups (Figures 1F and G). These results suggest that SHED-exos injected into SMGs increase saliva secretion and reduce lymphocytic infiltration in the SMGs of NOD mice.

SHED-exos are taken up by glandular epithelial cells

To investigate the distribution of SHED-exos, PKH-26-exos or DiR-exos were injected into the SMGs. We found that PKH-26-exos-positive signals were expressed intensively on the 1st day and appeared to be more uniformly distributed throughout the glandular tissues on the 3rd and 7th days (Figure 2A). In addition, DiR-exos were infused into the glands. As shown in Figures 2B-D, DiR-exos were distributed around the neck and precisely in the SMG. The heart, lung, liver, spleen, kidney, pancreas, and intestine tissues showed negative intensity (Figure 2E). Further observation showed that the positive signals in SMGs lasted for more than 40 days in 14-week-old mice (Figures 2F-J).

Next, we determined whether the exosomes were taken up by glandular epithelial cells. *In vitro*, PKH-26-exos were cultured with SMG-C6 cells, primary cultured acinar and duct cells of human SMG for 24 h. As shown in Figure 2K, there were positive signals in the cytoplasm of SMG-C6 cells, human acinar cells and duct cells, which suggest that SHED-exos can be ingested by salivary glandular epithelial cells to perform further functions.

SHED-exos upregulate the expression of the tight junction proteins ZO-1 and occludin

Fluid secretion can be accomplished through either the aquaporin 5 (AQP5)-mediated transcellular or tight junction-mediated paracellular route [25, 26]. We collected labial gland tissues from SS patients and found that the expression levels of AQP5, ZO-1, occludin, and claudin-4 were significantly decreased compared with those in controls. SHED-exos incubation with labial gland tissues from SS patients for 24 h remarkably increased the expression of ZO-1 and partially recovered the level of occludin but did not affect the contents of AQP5 and claudin-4 (Figures 3A-D). When SMG-C6 cells were cultured with SHED-exos for 24 h, the expression of ZO-1 and occludin was increased (Figures 3E-G). In addition, considering that the redistribution of tight junction proteins also affects their function, we further examined the location of ZO-1 and occludin. As shown in Figure 3H, SHED-exos did not change their distribution in SMG-C6 cells.

ZO-1 is required for the SHED-exo-induced increase in paracellular permeability

TER is an important indicator used to evaluate the function of tight junctions, and decreased TER is associated with increased paracellular permeability. In this study, the basal TER value of untreated SMG-

C6 monolayers was 589 ± 23.31 Ω cm^2, which was consistent with our previous studies [27]. SHED-exos induced a visible drop in TER values at 24 h and 48 h (Figures 3I). These results suggest that the therapeutic effect of SHED-exos in sialadenitis may involve enhancing ZO-1 and occludin expression and improving paracellular permeability in SMGs.

ZO-1 plays crucial roles in both basal salivary epithelial barrier function and paracellular transport [28]. To confirm that the increased paracellular permeability of SHED-exos was related to ZO-1, we conducted ZO-1 depletion and rescue experiments. Compared with control cells, ZO-1 protein expression markedly reduced in ZO-1 knockout cells and recovered in ZO-1 rescue cells (Figure 3J). Compared with the control cells, ZO-1 knockout did not affect the basic TER values, which was consistent with our previous study [28]. Furthermore, the decreased TER values induced by SHED-exos were abolished in ZO-1 knockout cells and reappeared in ZO-1 rescue cells (Figure 3K), which suggests that ZO-1 is required for the SHED-exo-induced increase in paracellular permeability.

The Akt/GSK-3β pathway mediates SHED-exo-induced ZO-1 expression and increased paracellular permeability

To explore the regulatory mechanism of SHED-exos on ZO-1, we performed a miRNA microarray of SHED-exos, and 180 exosomal miRNAs were identified and profiled, as shown in Table 1. KEGG pathway classification analysis was performed (Figure 4A left panel). The majority of the target genes mediating signal transduction were further listed in the right panel of Figure 4A, which suggested that the phosphatidylinositol 3 kinase (PI3K)-protein kinase B (PKB; Akt) pathway might play an important role. Moreover, in SHED-exo-treated SMGs of NOD mice, the ratios of p-Akt/Akt and p-GSK-3β/GSK-3β were decreased, but ZO-1 was increased (Figures 5A-E). *In vitro*, SHED-exos incubation for 24 h decreased the expression of p-Akt/Akt and p-GSK-3β/GSK-3β and increased the ZO-1 levels in SMG-C6 cells. Pretreatment with insulin-like growth factor 1 (IGF1), an Akt upstream molecule PI3K agonist, abolished SHED-exo-induced responses. IGF1 alone increased p-Akt/Akt and p-GSK-3β/GSK-3β expression but decreased ZO-1 expression (Figures 5F-J). These results suggest that Akt/GSK-3β signaling molecules negatively regulates ZO-1 expression and that SHED-exos increase ZO-1 expression *via* the Akt/GSK-3β pathway.

Furthermore, SHED-exos decreased the TER level, which could be attenuated by IGF1 preincubation. IGF1 treatment alone increased TER levels (Figure 4K). To further reveal whether ZO-1 was involved in the SHED-exo-induced increase in paracellular permeability *via* the Akt/GSK-3β pathway, a TER assay was performed on ZO-1 knockout cells. As shown in Figure 5L, SHED-exos- or IGF1-induced changes in the TER value disappeared in ZO-1 knockout SMG-C6 cells. These results suggest that the increased paracellular permeability induced by SHED-exos is related to Akt/GSK-3β pathway targeting at ZO-1.

Slug is involved in the SHED-exo-induced decrease in ZO-1

Slug, a Snail family transcription factor and the downstream signaling molecule of GSK-3β, is reported to act as a transcriptional repressor of several tight junction proteins, such as claudin-1, occludin, and ZO-1

in MDCK cells and claudin-3 in SMG-C6 cells [29, 30]. In the present study, SHED-exos decreased the Slug level in both SMG tissues (Figures 5A and D) and SMG-C6 cells (Figures 5M and N) but did not change Snail expression (Figures 5M-O). Moreover, IGF1 preincubation abolished the SHED-exo-induced Slug decrease and ZO-1 increase responses. IGF1 alone increased Slug expression but downregulated ZO-1 levels (Figures 5F and I-J). These results suggest that Slug acts as a transcriptional repressor of ZO-1 expression. To further reveal whether Slug binds to the ZO-1 gene directly, the promoter region of the rat ZO-1 gene was isolated and fused to the luciferase reporter vector. Transient transfection assays in the presence of pCMV6-Slug revealed that Slug significantly repressed wild-type ZO-1 promoter activity (Figure 5P). These results suggest that SHED-exos suppress Slug expression by inhibiting the Akt/GSK-3β pathway, thereby decreasing the transcriptional inhibition of Slug to ZO-1 and finally enhancing ZO-1 expression.

SHED-exo intraductal infusion into the SMG restores saliva secretion in NOD mice

Stem cell-based cell therapy is commonly performed using intravenous injection or local administration. For the exocrine glands, intraductal infusion is also a good choice. To facilitate the clinical application of SHED-exos, we infused SHED-exos through the orifice of the submandibular duct in 14-week-old NOD mice and collected the SMGs at 21 weeks. As shown in Figure 6A, DiR-exo intensities were observed in the neck area on the 1^{st} day and 14^{th} day after infusion and even on the 49^{th} day. As expected, the saliva flow rate was significantly increased in SHED-exo-infused mice compared with that in the PBS group (Figure 6B). After treatment, inflammatory cell infiltration in the SMG was alleviated. The focus scores and ratio index were decreased in the glands infused with SHED-exos compared with those in the PBS group (Figures 6C-E). Moreover, p-Akt/Akt, p-GSK-3β/GSK-3β, and Slug expression was decreased, and ZO-1 was increased in SHED-exo-infused glands compared with PBS controls (Figures 6F-J).

Discussion

In the present study, we demonstrated that local application of SHED-exos exhibited therapeutic benefits for sialadenitis induced by NOD. SHED-exos injected or infused into SMGs of NOD mice increased the saliva flow rate and alleviated glandular inflammation. Furthermore, SHED-exos improved paracellular permeability by elevating ZO-1 expression. A mechanistic study showed that inhibition of the Akt/GSK-3β pathway and a decrease in the transcriptional inhibition of Slug to ZO-1 were involved in promoting the secretion effect of SHED-exos (Figure 6K).

Recently, exosomes obtained from labial gland-derived stem cells were demonstrated to promote the proliferation of Treg cells, inhibit Th17 cells, ameliorate inflammatory infiltration in the exocrine glands and restore salivary gland secretory function in mouse models of SS [31]. In our previous study, intravenous injection of SHEDs exerted a protective effect on saliva secretion in the early phase of NOD mice by regulating T cell differentiation and improving the inflammatory microenvironment [10]. Here, we demonstrate that local injection of SHED-exos into the SMGs of 14-week-old NOD mice, a clinical phase of SS, significantly promotes salivary secretion and decreases lymphocytic infiltration in the SMGs of

NOD mice. Moreover, we demonstrated that intraductal infusion of SHED-exos into acinar units was an effective therapy for sialadenitis induced by NOD, which may provide a new feasible strategy to reduce the invasiveness of percutaneous needle injection and improve delivery to permeate the entire gland parenchyma. SHED-exos administered by local application could be taken up by salivary epithelial cells and lasted for more than 40 days.

Glandular epithelial cells are responsible for saliva secretion. Gland epithelial cells are the primary target of immune attack in SS, resulting in impaired expression, location, and function of secretion-related molecules, such as AQP5 and tight junction proteins [32, 33]. Tight junctions are protein complexes related to cell–cell interactions and play an essential role in regulating water and solute transport through the paracellular pathway in salivary glands [34, 35]. A previous study indicated that disruption of tight junction integrity and downregulation of ZO-1 and occludin were observed in minor salivary glands from SS patients [36]. Our previous study also showed that the elevated IL-17 in the SMGs of NOD mice impaired the expression of ZO-1, claudin-4, and their apicolateral membrane distribution through the NF-κB signaling pathway, which might contribute to salivary gland dysfunction in SS [37]. In the present study, ZO-1, occludin, and claudin-4 expression was decreased in the labial glands of SS patients, which indicated that the disruption in tight junction integrity was involved in decreased saliva secretion in SS. Local injection or perfusion of SHED-exos significantly increased ZO-1 expression in the salivary glands of NOD mice.

ZO-1 is an essential component in tight junction barrier function in submandibular epithelial cells, which links the membrane proteins of tight junctions to the actomyosin cytoskeleton and modulates the structure and function of tight junctions [28]. TER reflects the ions that pass through claudin-based charge-selective pores (~4 Å in radius) with instantaneous (typically in seconds) high permeability [38]. Knockout of ZO-1 did not change the base TER values, which was consistent with our previous study [28], confirming that ZO-1 alone did not obviously influence ionic permeability in normal salivary epithelium. However, SHED-exos incubation decreased TER values in SMG-C6 cells. These effects were abolished in ZO-1 knockout cells and recovered in ZO-1 rescued cells. These results indicate that SHED-exos increase the paracellular permeability of salivary gland epithelial cells *via* ZO-1, consequently enhancing gland secretory function.

Next, we focused on the regulatory mechanism of SHED-exos on ZO-1 expression. Based on the data from the exosomal miRNAs and KEGG analysis, we hypothesized that the PI3K-Akt pathway might contribute to the biological effect of SHED-exos. LY294002, a PI3K inhibitor, decreased B-lymphocyte viability in the labial glands of SS, which was deemed a future therapeutic option in SS [39]. Moreover, GSK-3 inhibitor-loaded osteotropic pluronic hydrogel was reported to reduce the chronic inflammatory state and the periodontal tissue damage associated with periodontitis [40]. The above studies suggest that the PI3K/Akt/GSK-3 pathway might be involved in regulating saliva secretion.

Previous studies showed that activation of PI3K/Akt pathway increased ZO-1, occludin, and claudin-1 expression, maintaining the normal barrier function of intestinal epithelial cells [41]. In contrast, in

cerebrovascular endothelial cells, activating the PI3K/Akt pathway decreased ZO-1 expression and function, destroyed the normal blood–brain barrier, and participated in the occurrence of ischemic stroke [42]. In this study, the ratios of p-Akt/Akt and p-GSK-3β/GSK-3β were decreased in SHED-exo-treated salivary glands and SMG-C6 cells, accompanied by increased ZO-1 expression and paracellular permeability. *In vitro*, activation of the Akt pathway by IGF1 decreased ZO-1 expression and paracellular permeability. IGF1 pretreatment also depressed the increased ZO-1 expression and paracellular permeability induced by SHED-exos. More importantly, the decreased paracellular permeability induced by IGF1 disappeared in ZO-1 knockout cells. These results suggest that the Akt/GSK-3β pathway negatively regulates ZO-1 expression. SHED-exos increase paracellular permeability by inhibiting Akt/GSK-3β pathway-mediated ZO-1 expression.

Slug, one of the Snail family proteins, is a key inducer of the epithelial-mesenchymal transition through mediating the transcriptional repression of tight junctions, adherens junctions, and desmosomes [43]. Our previous study showed that Slug activated by TNF-α can bind to claudin-3, thereby destroying the normal barrier function of epithelial cells in SMGs [29]. However, whether Slug can bind to ZO-1 and participate in saliva secretion is unknown. In this study, SHED-exos decreased Slug expression *in vivo* and *in vitro*, and the results from a double luciferase reporter gene assay directly confirmed that Slug could bind to the ZO-1 promotor and repress its activity. Activation of Akt can phosphorylate GSK-3β and inhibit its activity, thereby preventing the degradation of Slug, resulting in decreased expression of ZO-1, occludin, and E-cadherin in a study of renal function injury caused by ketamine [44]. In the present study, SHED-exos decreased the activation of the Akt/GSK-3β pathway. Dephosphorylation of GSK-3β might promote Slug degradation, thereby decreasing transcription inhibition of ZO-1.

Conclusions

In summary, we demonstrated that ZO-1 is a crucial target in mediating SHED-exo-modulated paracellular transport in the submandibular epithelium. SHED-exos increased ZO-1 expression and paracellular permeability of salivary cells by inhibiting the Akt/GSK-3/Slug pathway. Local application of SHED-exos significantly decreased SMG injury induced by SS. These findings enrich our understanding of the mechanism involved in SHED-exo-modulated saliva secretion and provide a potential therapeutic strategy for the local application of SHED-exos to sialadenitis induced by SS.

Abbreviations

SHEDs: Stem cells from human exfoliated deciduous teeth; SHED-exos: SHED-derived exosomes; SS: Sjögren syndrome; SMG: Submandibular glands; NOD: Nonobese diabetic; KEGG: Kyoto Encyclopedia of Genes and Genomes; MSCs: Mesenchymal stem cells; BMMSCs: Bone marrow-derived MSCs; SMG-C6: Submandibular epithelial cell line with characteristics of acinar cells; FBS: Fetal bovine serum; PBS: Phosphate-bufered saline; HSP70, Heat shock protein 70; AQP5, Aquaporin 5; ZO-1, Zonula occludens-1; NTA: Nanoparticle tracking analysis; DiR: The 1,1-dioctadecyl-3,3,3,3-tetramethylindotricarbocyanine iodide; TER: Transepithelial electrical resistance; PI3K: Phosphatidylinositol 3 kinase; Akt: protein kinase

B; p-Akt: Phospho-protein kinase B; GSK-3β: Glycogen synthase kinase-3β; p-GSK-3β: Phospho-glycogen synthase kinase3β; IGF1: Insulin-like growth factor 1; SD: Standard deviation.

Declarations

Acknowledgements

We thank Dr. David O. Quissell from School of Dentistry, University of Colorado Health Sciences Center, Denver, CO, USA, for the generous gift of rat SMG-C6 cell line.

Funding

This work was supported by the National Natural Science Foundation of China (Grand No. 81974151 and 81771088) and Peking University-Tason Stomatology Development Fund.

Availability of data and material

The datasets during and/or analysed during the current study available from the corresponding author on reasonable request.

Authors' contributions

ZD performed the experiments, analyzed the data and drafted the manuscript. PW and NJ analyzed the data, and draft the manuscript. LW interpreted the data, and critically revised the manuscript. CDand GYdesigned the study and critically revised the manuscript. All authors read, commented and approved the manuscript.

Ethics approval and consent to participate

Mice were used under the ethical approval and the ethical guidelines of the Peking University Institutional Review Board. Participate were informed about the research project, and informed consent forms were signed. The study was approved by the institutional review board of Peking University School of Stomatology.

Consent for publication

Not applicable.

Competing interests

The authors declare that they have no competing interests.

References

1. Nocturne G, Mariette X. Sjögren syndrome-associated lymphomas: an update on pathogenesis and management. Br J Haematol. 2015;168(3):317–27.
2. Brito-Zeron P, Acar-Denizli N, Zeher M, Rasmussen A, Seror R, Theander E, et al. Influence of geolocation and ethnicity on the phenotypic expression of primary Sjögren's syndrome at diagnosis in 8310 patients: a cross-sectional study from the big data Sjögren project consortium. Ann Rheum Dis. 2017;76(6):1042–50.
3. Haldorsen K, Moen K, Jacobsen H, Jonsson R, Brun JG. Exocrine function in primary Sjögren syndrome: natural course and prognostic factors. Ann Rheum Dis. 2008;67(7):949–54.
4. Anaya JM, Restrepo-Jimenez P, Rodriguez Y, Rodriguez-Jimenez M, Acosta-Ampudia Y, Monsalve DM, et al. Sjögren's syndrome and autoimmune thyroid disease: Two sides of the same coin. Clin Rev Allergy Immunol. 2019;56(3):362–74.
5. Ramos-Casals M, Tzioufas AG, Stone JH, Siso A, Bosch X. Treatment of primary Sjögren syndrome: a systematic review. JAMA. 2010;304(4):452–60.
6. Mariette X, Criswell LA. Primary Sjögren's syndrome. N Engl J Med. 2018;378(10):931–9.
7. Wong SK, Chin KY, Suhaimi FH, Fairus A, Ima-Nirwana S. Animal models of metabolic syndrome: A review. Nutr Metab (Lond). 2016;13:65.
8. Xu J, Wang D, Liu D, Fan Z, Zhang H, Liu O, et al. Allogeneic mesenchymal stem cell treatment alleviates experimental and clinical Sjögren syndrome. Blood. 2012;120(15):3142–51.
9. Matsumura-Kawashima M, Ogata K, Moriyama M, Murakami Y, Kawado T, Nakamura S. Secreted factors from dental pulp stem cells improve Sjögren's syndrome via regulatory T cell-mediated immunosuppression. Stem Cell Res Ther. 2021;12(1):182.
10. Du ZH, Ding C, Zhang Q, Zhang Y, Ge XY, Li SL, et al. Stem cells from exfoliated deciduous teeth alleviate hyposalivation caused by Sjögren syndrome. Oral dis. 2019;25(6):1530-44.
11. Kinnaird T, Stabile E, Burnett MS, Shou M, Lee CW, Barr S, et al. Local delivery of marrow-derived stromal cells augments collateral perfusion through paracrine mechanisms. Circulation. 2004;109(12):1543–9.
12. Ogata K, Katagiri W, Osugi M, Kawai T, Sugimura Y, Hibi H, et al. Evaluation of the therapeutic effects of conditioned media from mesenchymal stem cells in a rat bisphosphonate-related osteonecrosis of the jaw-like model. Bone. 2015;74:95–105.
13. Sugimura-Wakayama Y, Katagiri W, Osugi M, Kawai T, Ogata K, Sakaguchi K, et al. Peripheral nerve regeneration by secretomes of stem cells from human exfoliated deciduous teeth. Stem Cells Dev. 2015;24(22):2687–99.
14. Ogata K, Katagiri W, Hibi H. Secretomes from mesenchymal stem cells participate in the regulation of osteoclastogenesis in vitro. Clin Oral Investig. 2017;21(6):1979–88.
15. Kowal J, Arras G, Colombo M, Jouve M, Morath JP, Primdal-Bengtson B, et al. Proteomic comparison defines novel markers to characterize heterogeneous populations of extracellular vesicle subtypes. PNAS. 2016;113(8):E968-77.

16. van Niel G, Charrin S, Simoes S, Romao M, Rochin L, Saftig P, et al. The tetraspanin CD63 regulates ESCRT-independent and -dependent endosomal sorting during melanogenesis. Dev Cell. 2011;21(4):708–21.
17. Riazifar M, Mohammadi MR, Pone EJ, Yeri A, Lässer C, Segaliny AI, et al. Stem cell-derived exosomes as nanotherapeutics for autoimmune and neurodegenerative disorders. ACS Nano. 2019;13(6):6670–88.
18. Whiteside TL. Exosome and mesenchymal stem cell cross-talk in the tumor microenvironment. Semi Immunol. 2018;35:69–79.
19. Doeppner TR, Herz J, Gorgens A, Schlechter J, Ludwig AK, Radtke S, et al. Extracellular vesicles improve post-stroke neuroregeneration and prevent postischemic immunosuppression. Stem Cells Transl Med. 2015;4(10):1131–43.
20. Almazroa A, Sun W, Alodhayb S, Raahemifar K, Lakshminarayanan V. Optic disc segmentation for glaucoma screening system using fundus images. Clin Ophthalmol. 2017;11:2017–29.
21. Lonati C, Bassani GA, Brambilla D, Leonardi P, Carlin A, Maggioni M, et al. Mesenchymal stem cell-derived extracellular vesicles improve the molecular phenotype of isolated rat lungs during ischemia/reperfusion injury. J Heart Lung Transplant. 2019;38(12):1306–16.
22. Ding C, Cong X, Zhang Y, Yang NY, Li SL, Wu LL, et al. Hypersensitive mAChRs are involved in the epiphora of transplanted glands. J Dent Res. 2014;93(3):306–12.
23. Quissell DO, Barzen KA, Gruenert DC, Redman RS, Camden JM, Turner JT. Development and characterization of SV40 immortalized rat submandibular acinar cell lines. Vitro Cell Dev Biol Anim. 1997;33(3):164–73.
24. Yang WW, Yang LQ, Zhao F, Chen CW, Xu LH, Fu J, et al. Epiregulin promotes lung metastasis of salivary adenoid cystic carcinoma. Theranostics. 2017;7(15):3700–14.
25. Tsukita S, Furuse M, Itoh M. Multifunctional strands in tight junctions. Nat Rev Mol Cell Biol. 2001;2(4):285–93.
26. Mitic LL, Anderson JM. Molecular architecture of tight junctions. Annu Rev Physiol. 1998;60:121–42.
27. Ding C, Li L, Su YC, Xiang RL, Cong X, Yu HK, Li SL, Wu LL, Yu GY. Adiponectin increases secretion of rat submandibular gland via adiponectin receptors-mediated AMPK signaling. PLoS One. 2013 May;7(5):e63878. 8(.
28. Li J, Cong X, Zhang Y, Xiang RL, Mei M, Yang NY, et al. ZO-1 and -2 are required for TRPV1-modulated paracellular permeability. J Dent Res. 2015;94(12):1748–56.
29. Mei M, Xiang RL, Cong X, Zhang Y, Li J, Yi X, et al. Claudin-3 is required for modulation of paracellular permeability by TNF-alpha through ERK1/2/slug signaling axis in submandibular gland. Cell Signal. 2015;27(10):1915–27.
30. Ohkubo T, Ozawa M. The transcription factor Snail downregulates the tight junction components independently of E-cadherin downregulation. J Cell Sci. 2004;117(Pt 9):1675–85.

31. Li B, Xing Y, Gan Y, He J, Hua H. Labial gland-derived mesenchymal stem cells and their exosomes ameliorate murine Sjögren's syndrome by modulating the balance of Treg and Th17 cells. Stem Cell Res Ther. 2021;12(1):478.
32. Tsunawaki S, Nakamura S, Ohyama Y, Sasaki M, Ikebe-Hiroki A, Hiraki A, et al. Possible function of salivary gland epithelial cells as nonprofessional antigen-presenting cells in the development of Sjögren's syndrome. J Rheumatol. 2002;29(9):1884–96.
33. Mitsias DI, Kapsogeorgou EK, Moutsopoulos HM. The role of epithelial cells in the initiation and perpetuation of autoimmune lesions: lessons from Sjögren's syndrome (autoimmune epithelitis). Lupus. 2006;15(5):255–61.
34. Anderson JM. Molecular structure of tight junctions and their role in epithelial transport. News Physiol Sci. 2001;16:126–30.
35. Miyoshi J, Takai Y. Structural and functional associations of apical junctions with cytoskeleton. Biochim Biophys Acta. 2008;1778(3):670–91.
36. Ewert P, Aguilera S, Alliende C, Kwon YJ, Albornoz A, Molina C, et al. Disruption of tight junction structure in salivary glands from Sjögren's syndrome patients is linked to proinflammatory cytokine exposure. Arthritis Rheum. 2010;62(5):1280–9.
37. Zhang LW, Cong X, Zhang Y, Wei T, Su YC, Serrao AC, et al. Interleukin-17 impairs salivary tight junction integrity in sjögren's syndrome. J Dent Res. 2016;95(7):784–92.
38. Srinivasan B, Kolli AR, Esch MB, Abaci HE, Shuler ML, Hickman JJ. TEER measurement techniques for in vitro barrier model systems. J Lab Autom. 2015 Apr;20(2):107–26.
39. Rivière E, Pascaud J, Tchitchek N, Boudaoud S, Paoletti A, Ly B, Dupré A, Chen H, Thai A, Allaire N, Jagla B, Mingueneau M, Nocturne G, Mariette X. Salivary gland epithelial cells from patients with Sjögren's syndrome induce B-lymphocyte survival and activation. Ann Rheum Dis. 2020 Nov;79(11):1468–77.
40. Almoshari Y, Ren R, Zhang H, Jia Z, Wei X, Chen N, Li G, Ryu S, Lele SM, Reinhardt RA, Wang D. GSK3 inhibitor-loaded osteotropic Pluronic hydrogel effectively mitigates periodontal tissue damage associated with experimental periodontitis. Biomaterials. 2020 Dec;261:120293.
41. Zhuang Y, Wu H, Wang X, He J, He S, Yin Y. Resveratrol attenuates oxidative stress-induced intestinal barrier injury through PI3K/Akt-mediated Nrf2 signaling pathway. Oxid Med Cell Longev. 2019; 2019: 7591840.
42. Lv Y, Liu W, Ruan Z, Xu Z, Fu L. Myosin IIA regulated tight junction in oxygen glucose-deprived brain endothelial cells via activation of TLR4/PI3K/Akt/JNK1/2/14-3-3epsilon/NF-kappaB/MMP9 signal transduction pathway. Cell Mol Neurobiol. 2019;39(2):301-19.
43. Barrallo-Gimeno A, Nieto MA. The Snail genes as inducers of cell movement and survival: implications in development and cancer. Development. 2005;132(14):3151–61.
44. Lin Y, Zhang C, Xiang P, Shen J, Sun W, Yu H. Exosomes derived from HeLa cells break down vascular integrity by triggering endoplasmic reticulum stress in endothelial cells. J Extracell Vesicles. 2020;9(1):1722385.

Table

Table 1. Exosomal miRNAs profile in SHED-exos

No.	miRNAs	No.	miRNAs	No.	miRNAs
1	miR-8069	61	miR-4505	121	miR-6780b-5p
2	miR-7975	62	miR-1234-3p	122	miR-6085
3	miR-7977	63	miR-642b-3p	123	miR-6889-3p
4	miR-4516	64	miR-92a-3p	124	miR-6760-5p
5	miR-6089	65	miR-642a-3p	125	miR-1229-5p
6	miR-5100	66	miR-3663-3p	126	miR-320b
7	miR-6087	67	miR-320d	127	miR-320a
8	miR-6090	68	miR-6724-5p	128	miR-1825
9	miR-4299	69	miR-3665	129	miR-513a-5p
10	miR-4281	70	miR-7110-5p	130	miR-4749-3p
11	miR-1260a	71	miR-23a-3p	131	miR-4787-3p
12	miR-4459	72	miR-1228-3p	132	miR-8063
13	miR-4286	73	miR-130a-3p	133	miR-4484
14	miR-3960	74	miR-6124	134	miR-6777-3p
15	miR-6869-5p	75	miR-4687-3p	135	miR-574-5p
16	miR-6125	76	miR-3162-3p	136	miR-425-3p
17	miR-1246	77	miR-320e	137	miR-6785-5p
18	miR-4530	78	miR-6803-5p	138	miR-4515
19	miR-7641	79	miR-6819-3p	139	miR-5001-5p
20	miR-630	80	miR-6797-3p	140	miR-4763-3p
21	miR-6800-5p	81	miR-6069	141	miR-193a-5p
22	miR-5787	82	miR-6165	142	miR-6848-3p
23	miR-1273g-3p	83	miR-1915-3p	143	miR-6760-3p
24	miR-5703	84	let-7a-5p	144	miR-6727-5p
25	miR-3679-5p	85	miR-29a-3p	145	miR-7114-3p
26	miR-1260b	86	hsa-miR-671-5p	146	miR-4769-3p
27	miR-7150	87	miR-1238-3p	147	miR-5006-5p
28	miR-6821-5p	88	miR-4485-3p	148	miR-4787-5p

No.	miRNAs	No.	miRNAs	No.	miRNAs
29	miR-6127	89	miR-4507	149	miR-371b-5p
30	miR-22-3p	90	miR-7704	150	miR-4746-3p
31	miR-2861	91	miR-1587	151	miR-6795-3p
32	miR-638	92	miR-6068	152	miR-6763-3p
33	miR-6763-5p	93	miR-1304-3p	153	miR-4271
34	miR-940	94	miR-6800-3p	154	let-7c-5p
35	miR-320c	95	miR-4284	155	miR-6824-3p
36	miR-4741	96	miR-6508-5p	156	miR-6861-3p
37	miR-197-5p	97	miR-6737-3p	157	miR-423-5p
38	miR-575	98	miR-6740-5p	158	miR-636
39	miR-6088	99	miR-6515-3p	159	miR-6765-3p
40	miR-1290	100	miR-6076	160	miR-6126
41	miR-6510-5p	101	miR-4313	161	miR-4323
42	miR-6826-5p	102	miR-4433a-5p	162	miR-6785-3p
43	miR-6749-5p	103	miR-6891-5p	163	miR-1275
44	miR-5739	104	miR-3196	164	miR-6766-3p
45	miR-100-5p	105	miR-6851-3p	165	miR-4257
46	miR-221-3p	106	miR-6875-5p	166	miR-324-3p
47	miR-494-3p	107	miR-125b-5p	167	miR-4767
48	miR-1268a	108	miR-4725-5p	168	miR-1229-3p
49	miR-4665-3p	109	miR-191-3p	169	miR-4758-3p
50	miR-3162-5p	110	miR-6813-3p	170	miR-6796-3p
51	miR-1207-5p	111	miR-762	171	miR-4652-3p
52	let-7b-5p	112	miR-1237-3p	172	miR-4656
53	miR-4466	113	miR-328-5p	173	miR-6870-3p
54	miR-6879-5p	114	miR-4649-3p	174	miR-6812-3p
55	miR-3656	115	miR-4443	175	miR-6731-3p
56	miR-21-5p	116	miR-1268b	176	miR-3180-5p

No.	miRNAs	No.	miRNAs	No.	miRNAs
57	miR-4485-5p	117	miR-6880-3p	177	miR-4750-3p
58	miR-1202	118	miR-1281	178	miR-6798-3p
59	miR-1225-5p	119	miR-125a-3p	179	miR-766-3p
60	miR-7107-5p	120	miR-1908-3p	180	miR-933

Figures

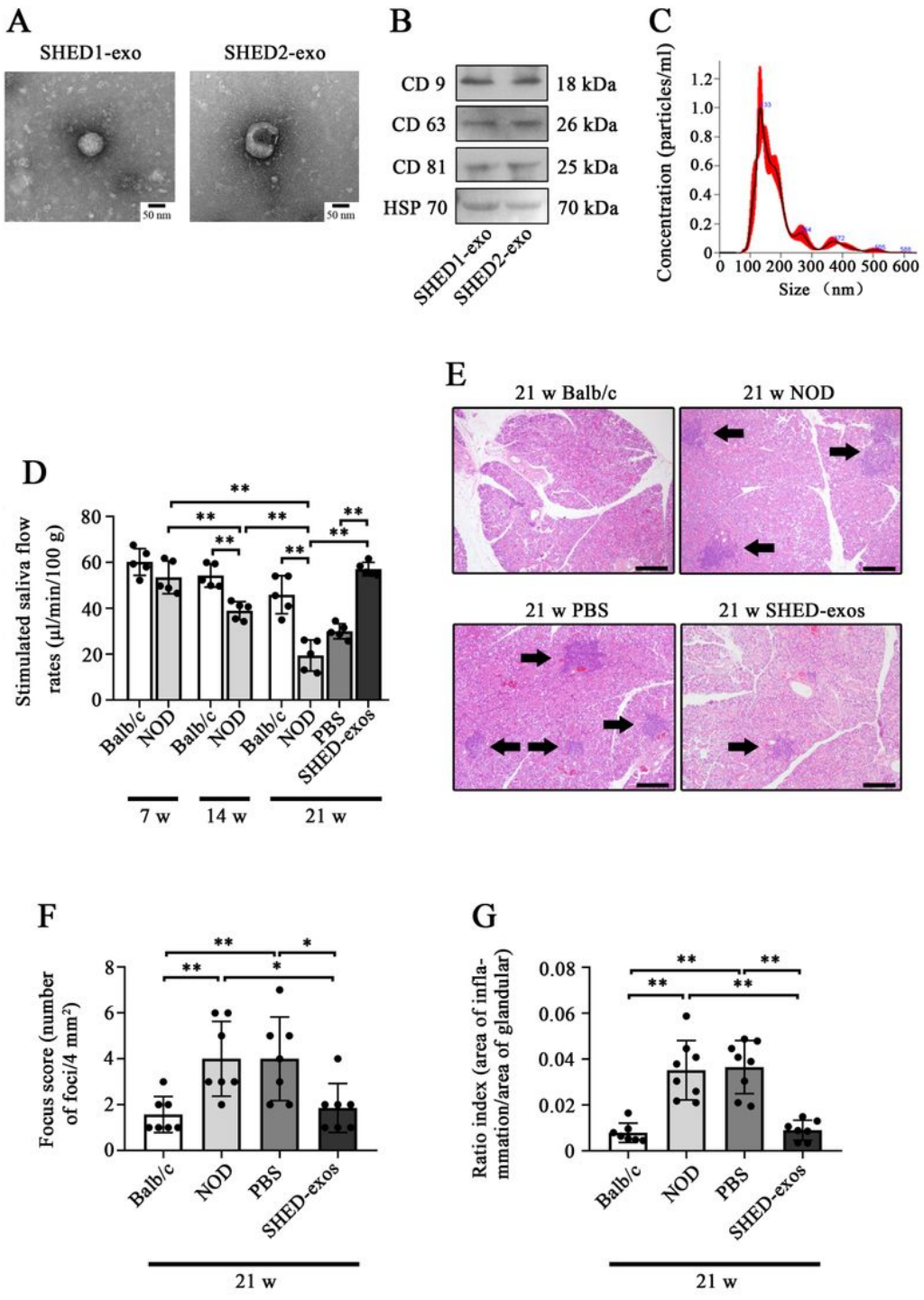

Figure 1

SHED-exos increased the saliva secretion and ameliorated lymphocytic infiltration in the SMG of NOD mice. A, The microstructure of SHED-exos. **B**, The expressions of CD9, CD63, CD81, and HSP70 in SHED-exos. **C**, The size distribution and particle concentration of SHED-exos. **D**, SHED-exos (50 μg in 25 μl PBS per side) and PBS control were injected into the SMGs of 14-week-old NOD mice, respectively. The stimulated saliva flow rates were measured at 21 weeks. **E**, The histological appearances of SMGs in 21-

week-old Balb/c mice and NOD mice with or without SHED-exos injection. Inflammatory cell foci are shown with arrows. Scale bar, 200 μm. **F** and **G**, The degree of inflammatory infiltration in the SMGs of NOD mice was evaluated by the focus score and the ratio index. Bars show the mean ± SD (n = 5). * $P < 0.05$, ** $P < 0.01$.

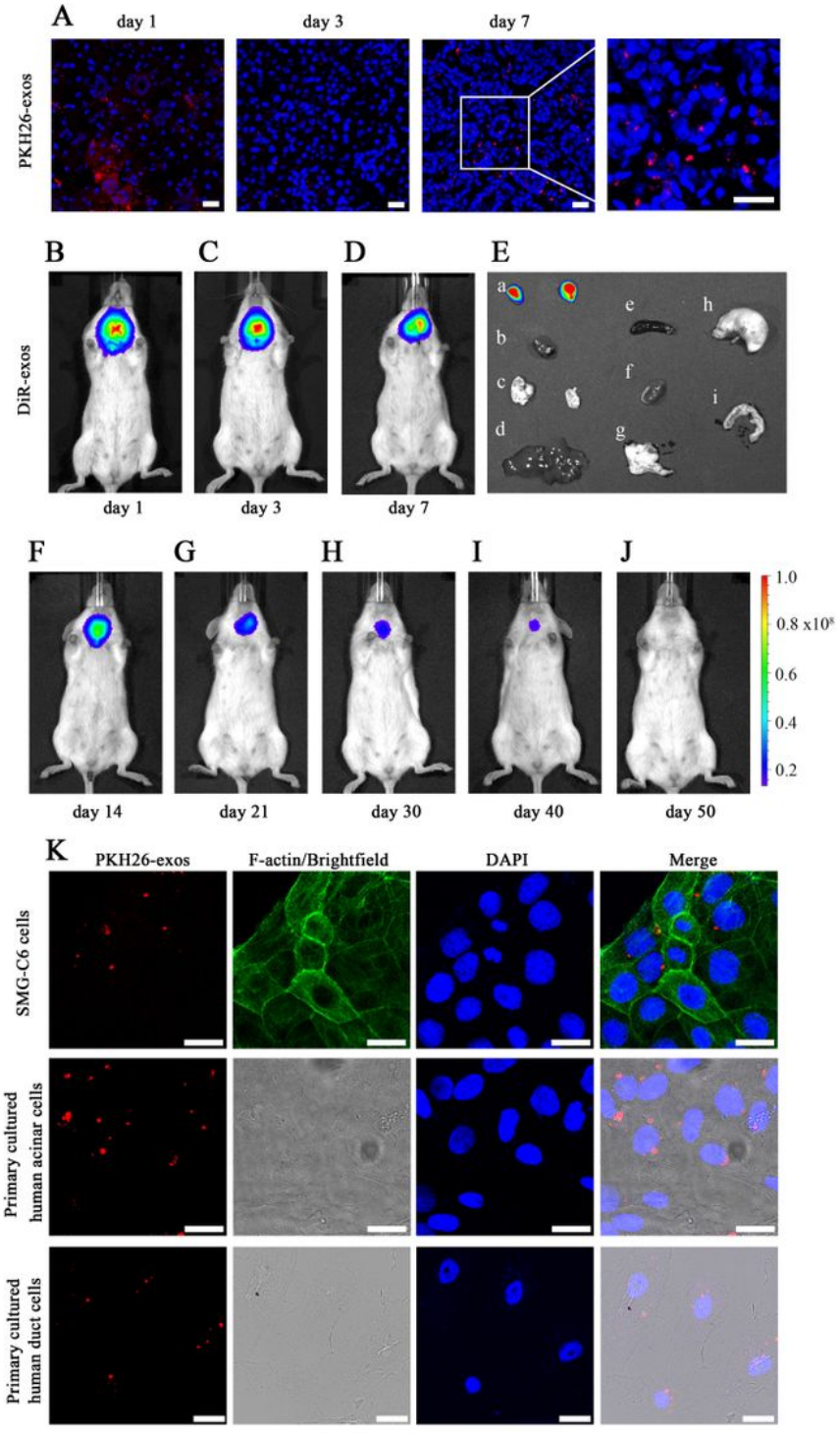

Figure 2

SHED-exos are taken up by glandular epithelial cells. A, Representative appearances of SMGs on the 1st, 3rd, 7th day after PKH26-exos (red) injection, respectively. Scale bar, 200 μm. Nuclei were stained with DAPI (blue). **B-D,** Bioluminescence was detected on the1st, 3rd, 7th day after injection of DiR-exos. **E,** Organs were harvested and detected on the 7th day. a. SMG; b. heart; c. lung; d. liver; e. spleen; f. kidney; g. pancreas tissue; h. stomach; i. intestines. **F-J,** Bioluminescence was detected on the 14th, 21st, 30th, 40th, 50th day after injection of DiR-exos. **K,** The uptake of PKH26-exos (red) by SMG-C6 cells, primary cultured human SMG acinar and duct cells. DAPI (blue), F-actin (green). Scale bar, 200 μm.

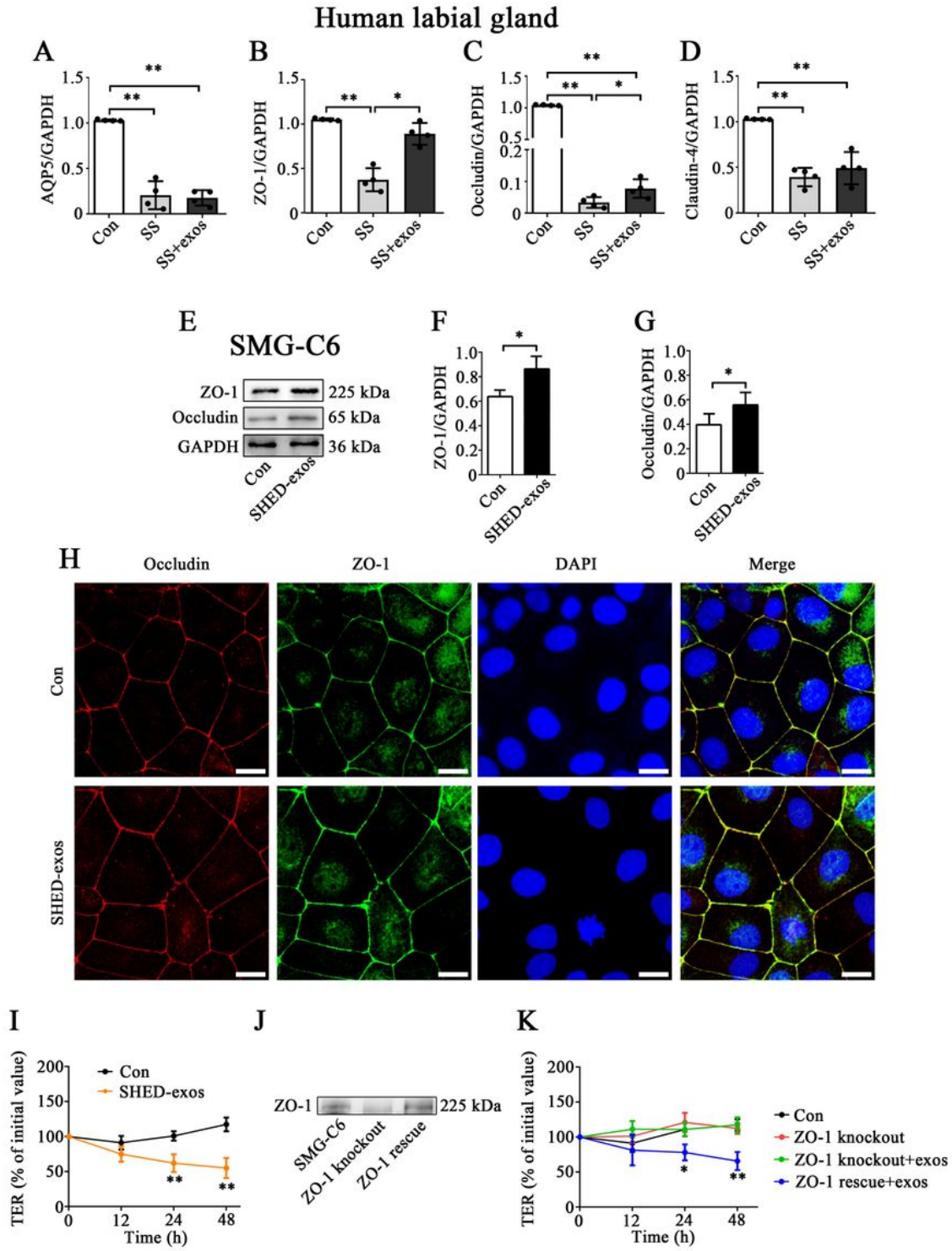

Figure 3

SHED-exos upregulate ZO-1 expressions and increased paracellular permeability in ZO-1 dependent manner. A-D, mRNA expressions of AQP5, ZO-1, occludin, and claudin-4 in control gland and SS labial gland with or without stimulation with SHED-exos. **E,** Expressions of ZO-1 and occludin in SMG-C6 cells stimulated with 200μg/ml SHED-exos for 24 h. **F and G,** Quantitative analysis of ZO-1 and occludin expressions normalized to GAPDH. **H,** The distribution of ZO-1 and occludin were examined in SMG-C6

cells with or without SHED-exos. ZO-1 (red), occludin (green), DAPI (blue). Scale bar, 20 μm. **I,** The effects of SHED-exos on TER in SMG-C6 cells. **J,** ZO-1 expression in ZO-1 knockout cells and "rescued" cells. **K,** The effects of SHED-exos on TER in control, ZO-1 knockout, and ZO-1 rescued SMG-C6 cells. Bars show the mean ± SD (n = 4). * $P < 0.05$, ** $P < 0.01$.

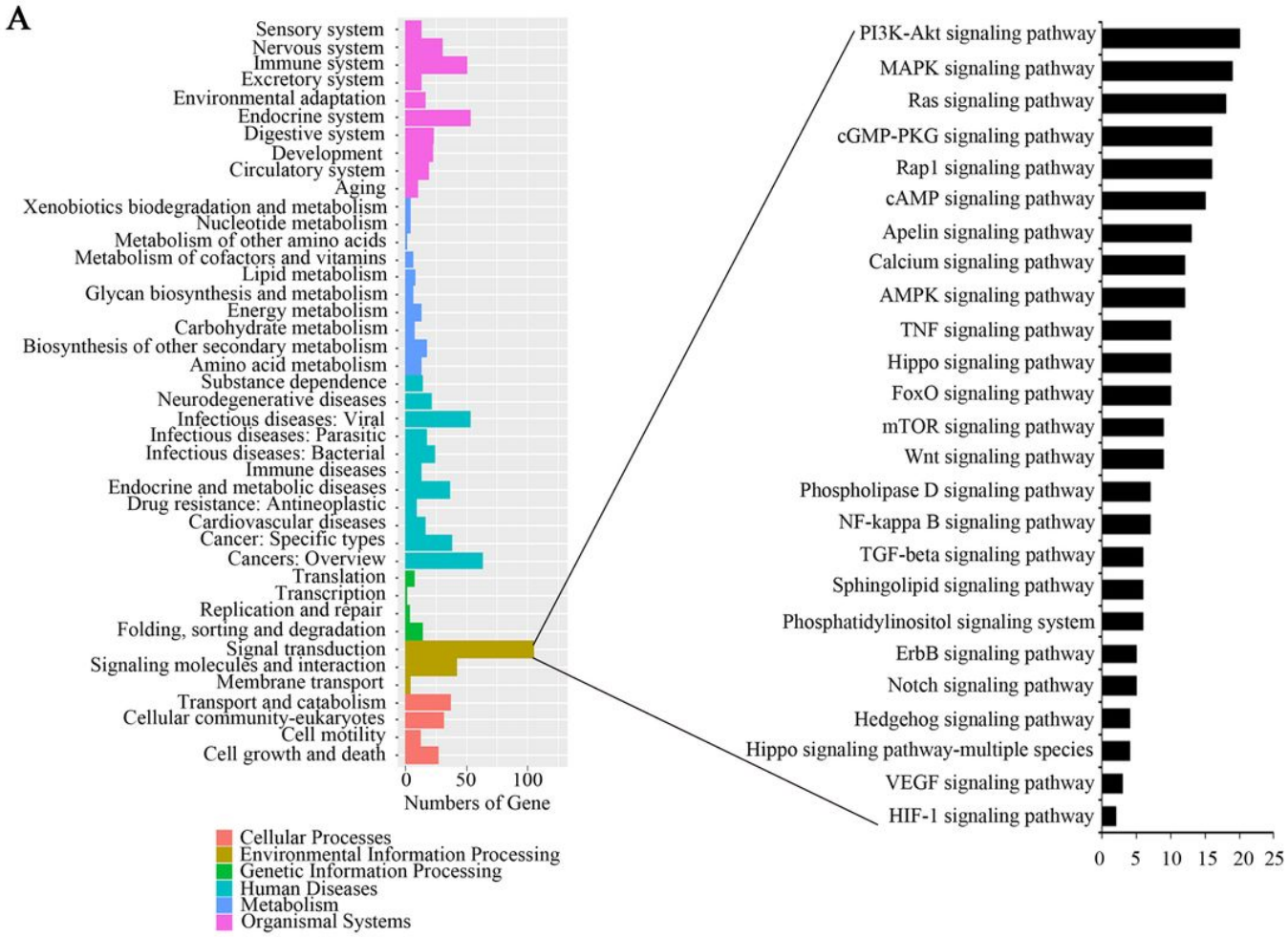

Figure 4

The Akt/GSK-3β/ expressions in NOD mice. A, Signaling pathway analysis from KEGG pathway classification of exosamal miRNAs target genes.

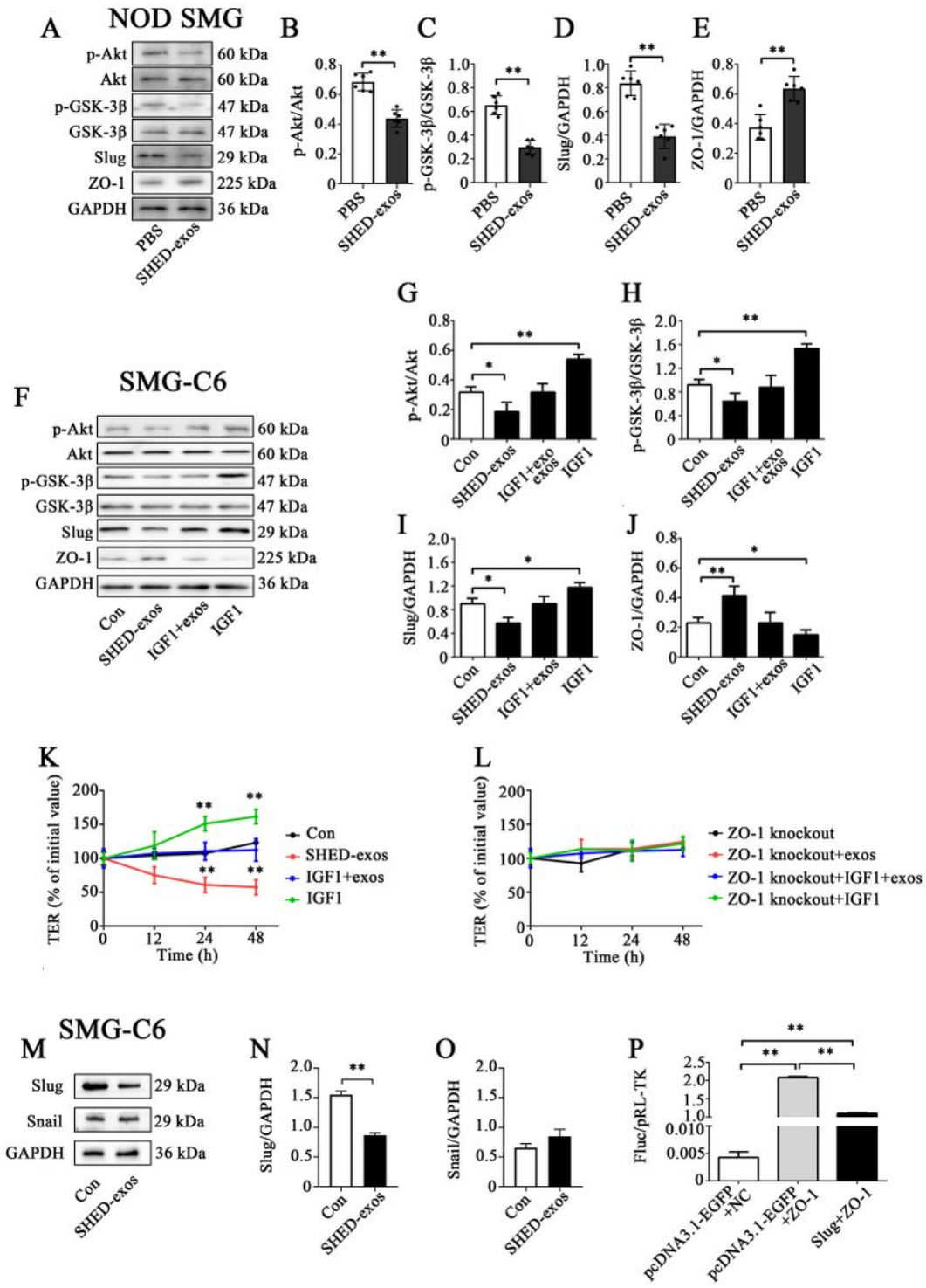

Figure 5

SHED-exos regulated ZO-1 expression *via* Akt/GSK-3β/Slug pathway. A, Expressions of p-Akt, Akt, p-GSK-3β, GSK-3β, Slug, and ZO-1 in SHED-exos treated gland**. B-E**, Quantitative analysis of p-Akt/Akt, p-GSK-3β/GSK-3β, Slug/GAPDH, and ZO-1/GAPDH. **F**, Expressions of p-Akt, Akt, p-GSK-3β, GSK-3β, Slug, and ZO-1 in SMG-C6 cells treated with SHED-exos, pre-incubated with 100 ng/ml IGF1 for 1 h, and then SHED-exos for 24 h, and IGF1 alone**. G-J,** Quantitative analysis of p-Akt/Akt, p-GSK-3β/GSK-3β, Slug/GAPDH,

and ZO-1/GAPDH. **K,** The effects of SHED-exos on TER in the four groups**. L**, The effects of SHED-exos on TER on ZO-1 knockout cells**. M-O**, The Slug and Snail expressions in SHED-exos treated cells. **P**, Slug binded to ZO-1 promoter and suppress its transcription. Bars show the mean ± SD (n = 6). * *P* < 0.05, ** *P* < 0.01.

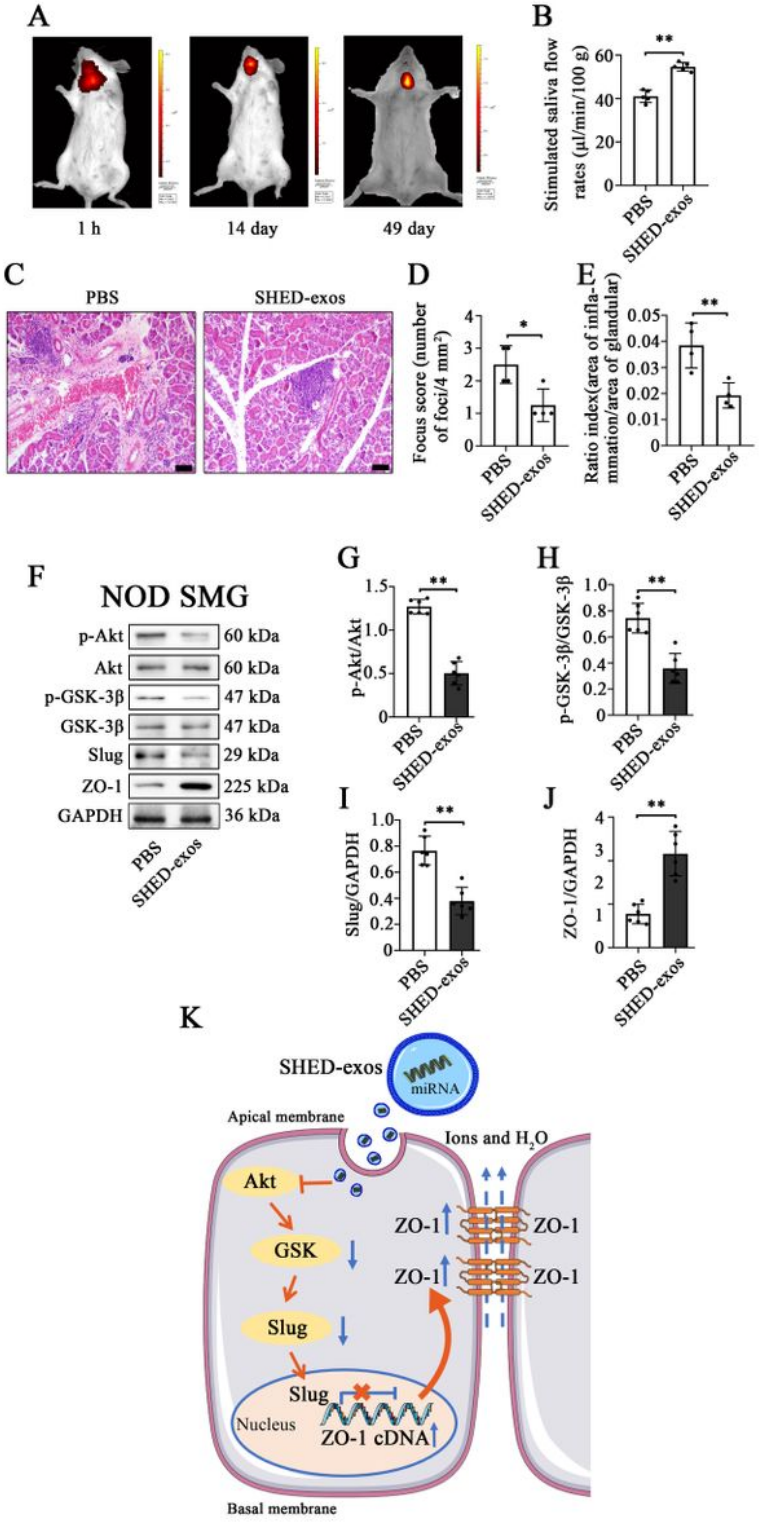

Figure 6

Intraductal infusion with SHED-exos. A, Bioluminescence was detected on the1st, 14th, 49th day after intraductal injection of DiR-exos. **B**. The stimulated saliva flow rates were measured and analysed at 21 weeks. **C**, Representative histological appearances of SMGs in 21-week-old NOD mice with or without SHED-exos treatment. Inflammatory cell foci were shown with arrows. Scale bar, 200 μm. **D** and **E**, The degree of inflammatory infiltration in the SMG of NOD mice was evaluated by the focus score and the ratio index. **F,** Expressions of p-Akt, Akt, p-GSK-3β, GSK-3β, Slug, and ZO-1 in SHED-exos treated gland**. G-I**, Quantitative analysis of p-Akt normalized to Akt, p-GSK-3β normalized to GSK-3β, Slug and ZO-1 normalized to GAPDH. **K,** Schematic illustration showing the mechanism of SHED-exos increased paracellular permeability of salivary gland cells via Akt/GSK-3β/Slug-mediated ZO-1 expression. Bars show the mean ± SD (n = 4). *P < 0.05, **P < 0.01.

Supplementary Files

This is a list of supplementary files associated with this preprint. Click to download.

- additionalfile1.doc